April 27, 2016

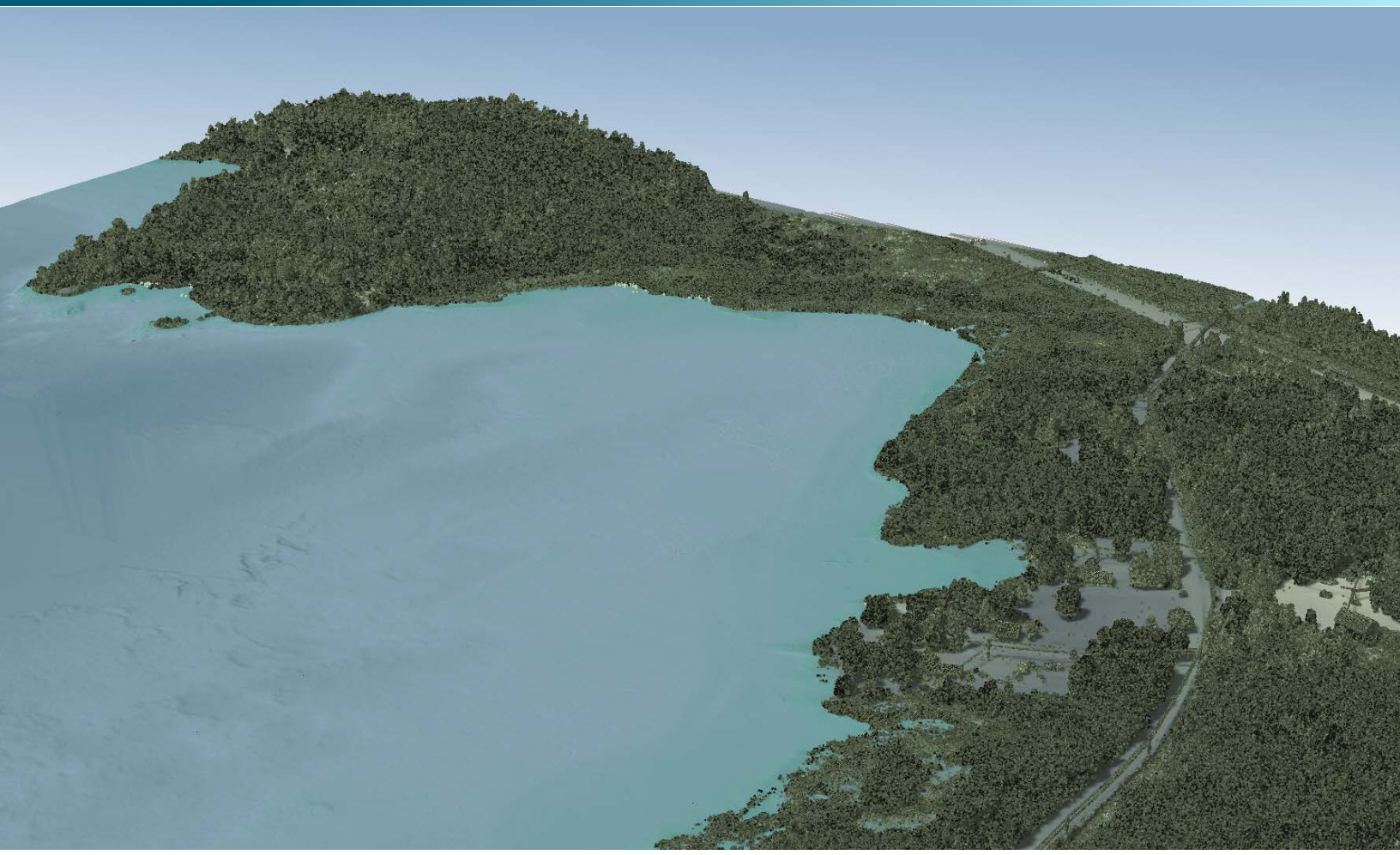

St. Marys River Topobathymetric LiDAR

Technical Data Report

US Army Corps of Engineers

Kevin Ryan
US Army Corps of Engineers
EC-S
1222 Spruce Street
St. Louis, Missouri 63103
PH: 603-646-4106

QSI Corvallis
517 SW 2nd St., Suite 400
Corvallis, OR 97333
PH: 541-752-1204

TABLE OF CONTENTS

Cover Photo: A view looking northwest over Hay Bay. The image was created from the gridded LiDAR surface colored by elevation and overlaid with the 3D point cloud.

INTRODUCTION

This photo taken by QSI acquisition staff shows a view of static GNSS equipment set up over monument ST_MARYS_06 in the St. Marys River site in Ontario, Canada.

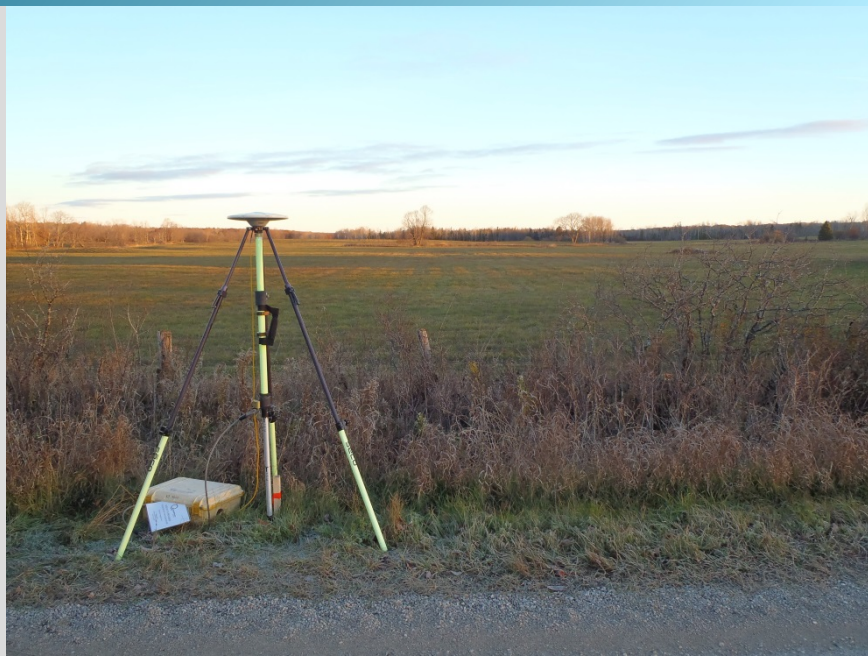

In September 2015, Quantum Spatial (QSI) was contracted by the United States Army Corps of Engineers (USACE) to collect topobathymetric Light Detection and Ranging (LiDAR) data in the fall of 2015 for selected areas of the St. Marys River in Michigan and Ontario, Canada. Traditional near-infrared (NIR) LiDAR was fully integrated with green wavelength return data (bathymetric) LiDAR in order to provide seamless and complete project mapping. Data were collected to aid USACE in assessing the topographic and geophysical properties (channel morphology and topobathymetric surface) of the study area.

This report accompanies the delivered topobathymetric LiDAR data and documents contract specifications, data acquisition procedures, processing methods, and analysis of the final dataset including LiDAR accuracy, depth penetration, and density. Acquisition dates and acreage are shown in Table 1, the project extent is shown in Figure 1, and a complete list of contracted deliverables provided to USACE is shown in Table 2.

Table 1: Acquisition dates, acreage, and data types collected on the St. Marys River sites

Project Site	Contracted Acres	Buffered Acres	Acquisition Dates	Data Type
St. Marys River	86,400	127,614	10/9/2015 - 11/29/2015	LiDAR

Deliverable Products

Table 2: Products delivered to USACE for the St. Marys River sites

St. Marys River Products Projection: Michigan State Plane North Horizontal Datum: NAD83 (2011) Vertical Datum: NAVD88 (GEOID12B) Units: Meters	
Topobathymetric LiDAR	
Points	LAS v 1.2 • All Returns • Model Keypoints
Rasters	1.0 Meter ESRI Grids • Topographic Bare Earth Model • Bathymetric Bare Earth Model • Integrated Topobathymetric Model • Integrated Topobathymetric Model of Model Key Points 0.5 Meter GeoTiffs • NIR Intensity Images • Green wavelength Intensity Images
Vectors	Shapefiles (*.shp) • Site Boundary • LiDAR Tile Index • DEM Tile Index • Flightlines • Contours (0.5m) • Water Breaklines • Bathymetric Void Shape • Survey Control Points
InRoads DTM	• InRoads Digital Terrain Models (*.dtm)

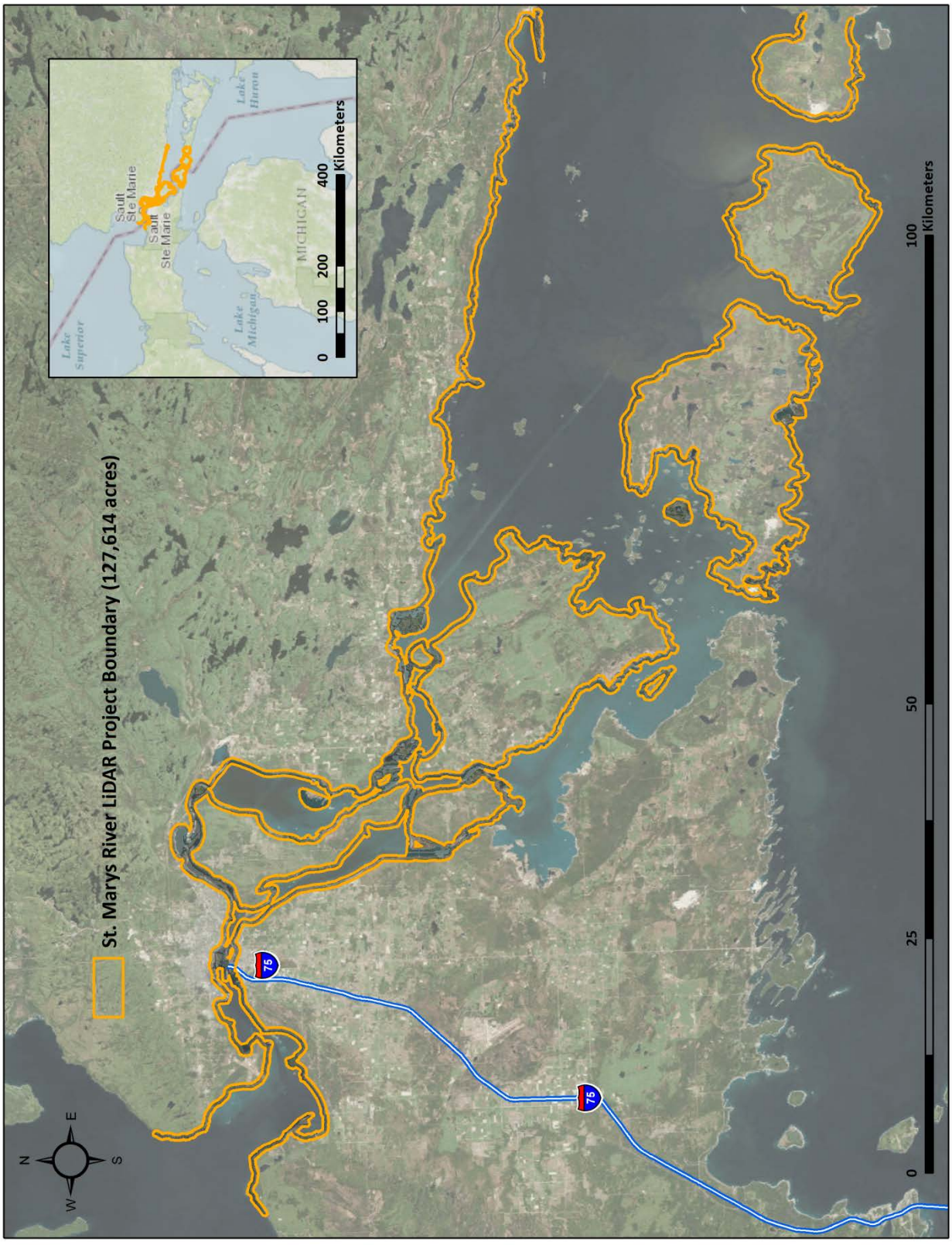

Figure 1: Location map of the St. Marys River site

QSI's Cessna Caravan 208B

Bathymetric Sensor Selection: the Riegl VQ-820-G

The Riegl VQ-820-G was selected as the hydrographic airborne laser scanner for the St. Marys River project based on fulfillment of several considerations deemed necessary for effective mapping of the project site. A high repetition pulse rate, high scanning speed, small laser footprint, and wide field of view allow for seamless collection of high resolution data of both topographic and bathymetric surfaces. A short laser pulse length allows for discrimination of underwater surface expression in shallow water, critical to shallow and dynamic environments. The Riegl system has demonstrated hydrographic depth ranging capability up to 1 Secchi depth on bright reflective surfaces. Sensor specifications and settings for the St. Marys River acquisition are displayed in Table 6.

Planning

In preparation for data collection, QSI reviewed the project area and developed a specialized flight plan to ensure complete coverage of the St. Marys River LiDAR study area at the target point density of ≥4.0 points/m^2 for green LiDAR returns, and ≥6.0 points/m^2 for NIR LiDAR returns (determined by the altitude required for flying topo-bathymetry). Acquisition parameters including orientation relative to terrain, flight altitude, pulse rate, scan angle, and ground speed were adapted to optimize flight paths and flight times while meeting all contract specifications.

Factors such as satellite constellation availability and weather windows must be considered during the planning stage. Any weather hazards or conditions affecting the flight were continuously monitored due to their potential impact on the daily success of airborne and ground operations. In addition, logistical considerations including private property access and potential air space restrictions, and river flow rates (Figure 2 and Figure 3), and water clarity were reviewed.

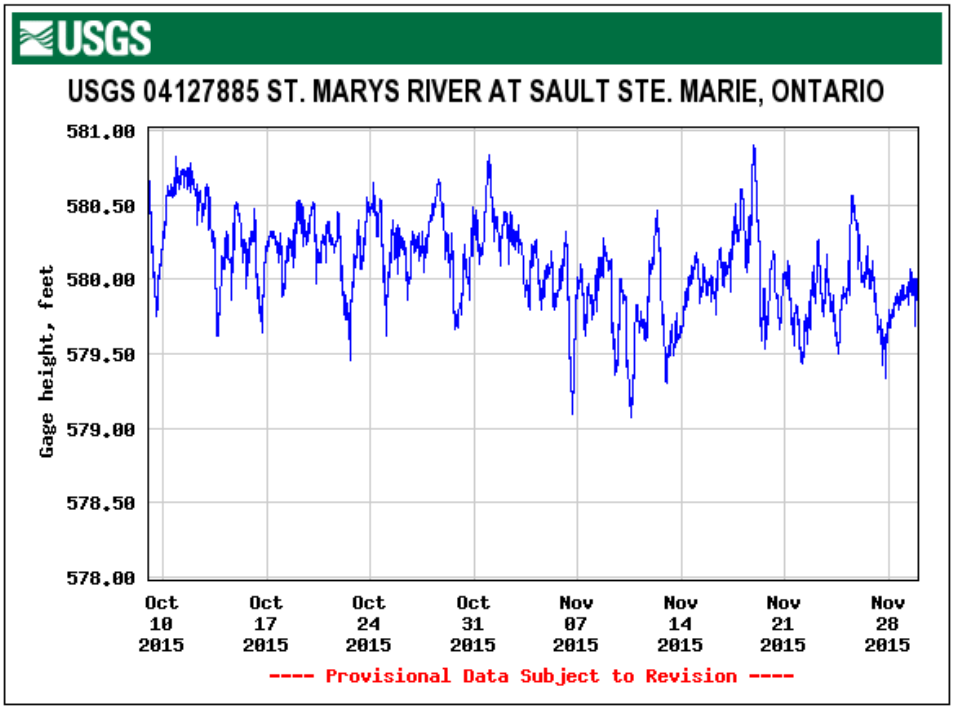

Figure 2: USGS Station 04127885 gauge height along the St. Marys River at the time of LiDAR acquisition.

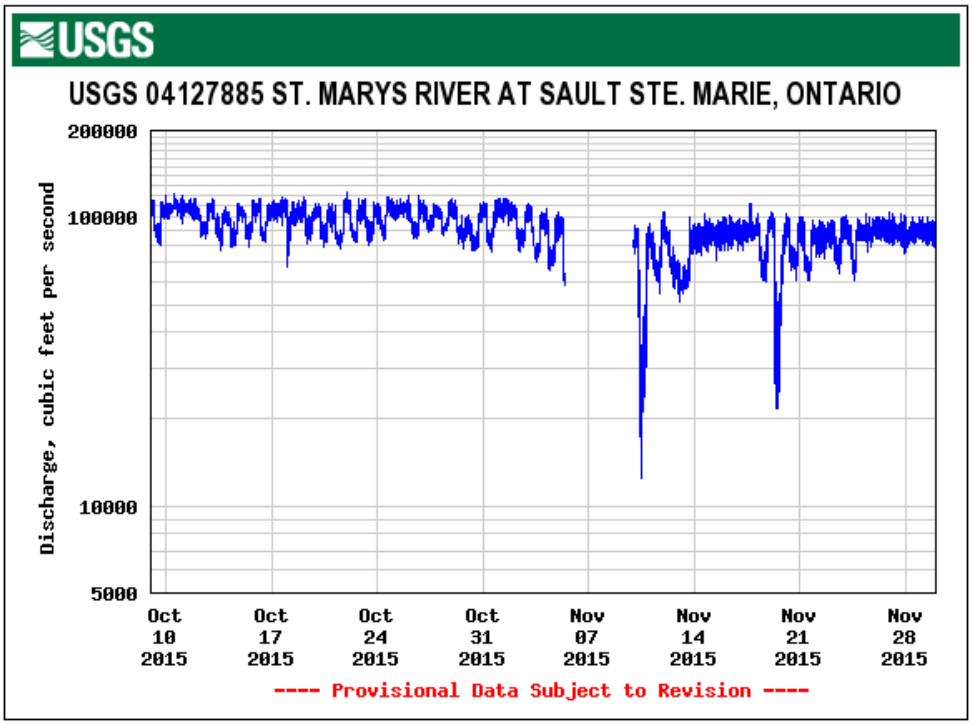

Figure 3: USGS Station 04127885 flow rates along the St. Marys River at the time of LiDAR acquisition.

This photo taken by QSI acquisition staff displays water clarity conditions in Drummond Township Park

Airborne Survey

LiDAR

The LiDAR survey was accomplished using a Leica ALS50 system dually mounted with a Riegl VQ-820-G topobathymetric sensor in a Cessna Caravan 208B. The Riegl VQ-820-G uses a green wavelength (λ=532 nm) laser that is capable of collecting high resolution vegetation and topography data, as well as penetrating the water surface with minimal spectral absorption by water. The recorded waveform enables range measurements for all discernible targets for a given pulse. The typical number of returns digitized from a single pulse range from 1 to 7 for the St. Marys River project area. The Leica ALS50 laser system records up to four range measurements (returns) per pulse. It is not uncommon for some types of surfaces (e.g., dense vegetation or water) to return fewer pulses to the LiDAR sensor than the laser originally emitted. The discrepancy between first return and overall delivered density will vary depending on terrain, land cover, and the prevalence of water bodies. All discernible laser returns were processed for the output dataset. Table 3 summarizes the settings used to yield an average pulse density of ≥4.0 points/m^2 for green LiDAR returns and ≥6.0 points/m^2 for NIR LiDAR returns over the St. Marys River project area.

Table 3: LiDAR specifications and survey settings

LiDAR Survey Settings & Specifications		
Sensor	**Leica ALS50**	**Riegl VQ-820G**
Acquisition Dates	10/9/2015 – 10/12/15, 10/17/15, 10/18/15, 10/25/15, 10/26/15, 10/30/15, 11/2/15, 11/4/15, 11/5/15, 11/8/15, 11/9/15, 11/11/15, 11/14/15 – 11/17/15, 11/20/15, 11/21/15, 11/24/15, 11/25/15, 11/28/15, 11/29/15	10/9/2015 – 10/12/15, 10/17/15, 10/18/15, 10/25/15, 10/26/15, 10/30/15, 11/2/15, 11/4/15, 11/5/15, 11/8/15, 11/9/15, 11/11/15, 11/14/15 – 11/17/15, 11/20/15, 11/21/15, 11/24/15, 11/25/15, 11/28/15, 11/29/15
Aircraft Used	Cessna Caravan 208B	Cessna Caravan 208B
Survey Altitude (AGL)	400m	400m
Target Pulse Rate	150 kHz	284 kHz
Pulse Mode	Single Pulse in Air (SPiA)	Single Pulse in Air (SPiA)
Laser Pulse Footprint Diameter	10 cm	40 cm
Mirror Scan Rate	42.9 Hz	50 – 200 Hz
Field of View	44°	42°
GPS Baselines	≤13 nm	≤13 nm
GPS PDOP	≤3.0	≤3.0
GPS Satellite Constellation	≥6	≥6
Maximum Returns	4	Unlimited
Intensity	8-bit (Scaled to 16-bit)	16-bit
Resolution/Density	Average 6 pulses/m^2	Average 4 pulses/m^2
Accuracy	$RMSE_Z$ ≤ 15 cm	RMSEZ ≤ 15 cm

All areas were surveyed with an opposing flight line side-lap of ≥50% (≥100% overlap) in order to reduce laser shadowing and increase surface laser painting. To accurately solve for laser point position (geographic coordinates x, y and z), the positional coordinates of the airborne sensor and the attitude of the aircraft were recorded continuously throughout the LiDAR data collection mission. Position of the aircraft was measured twice per second (2 Hz) by an onboard differential GPS unit, and aircraft attitude was measured 200 times per second (200 Hz) as pitch, roll and yaw (heading) from an onboard inertial measurement unit (IMU). To allow for post-processing correction and calibration, aircraft and sensor position and attitude data are indexed by GPS time.

Ground Control

Ground control surveys, including monumentation, and ground survey points (GSPs), were conducted to support the airborne acquisition. Ground control data were used to geospatially correct the aircraft positional coordinate data and to perform quality assurance checks on final LiDAR data.

QSI-Established Monument ST_MARYS_04

Monumentation

The spatial configuration of ground survey monuments provided redundant control within 13 nautical miles of the mission areas for LiDAR flights. Monuments were also used for collection of ground survey points using real time kinematic (RTK) and post processed kinematic (PPK) survey techniques.

Monument locations were selected with consideration for satellite visibility, field crew safety, and optimal location for GSP coverage. QSI utilized three existing monuments and established twenty new monuments for the St. Marys River LiDAR project (Table 4,Figure 4). New monumentation was set using 5/8” x 30” rebar topped with stamped 2 1/2" aluminum caps.

Table 4: Monuments established for the St. Marys River acquisition. Coordinates are on the NAD83 (2011) datum, epoch 2010.00

Monument ID	Latitude	Longitude	Ellipsoid (meters)
RH0077	46° 00' 35.77390"	-83° 44' 22.73677"	162.886
RH0078	46° 00' 31.35144"	-83° 44' 42.28129"	163.808
RJ0586	46° 29' 02.31104"	-84° 37' 56.45303"	151.324
ST_MARYS_01	45° 55' 51.23134"	-83° 32' 36.52976"	146.603
ST_MARYS_02	46° 28' 52.47072"	-84° 21' 51.27084"	182.207
ST_MARYS_03	46° 17' 18.06501"	-83° 36' 42.76729"	143.36
ST_MARYS_04	46° 15' 26.83263"	-83° 28' 25.74193"	149.001
ST_MARYS_05	45° 54' 46.65526"	-83° 07' 21.64041"	155.528
ST_MARYS_06	45° 54' 45.08935"	-83° 09' 21.97469"	165.142
ST_MARYS_07	46° 12' 30.42899"	-83° 09' 15.58371"	153.917

Monument ID	Latitude	Longitude	Ellipsoid (meters)
ST_MARYS_08	46° 14' 28.30226"	-83° 19' 16.49826"	163.667
ST_MARYS_09	46° 20' 32.18688"	-83° 53' 28.97440"	143.392
ST_MARYS_10	46° 11' 16.11807"	-83° 49' 20.78931"	144.751
ST_MARYS_11	46° 15' 39.33378"	-84° 00' 45.89162"	170.63
ST_MARYS_12	46° 31' 18.87329"	-84° 24' 34.76945"	153.482
ST_MARYS_13	46° 32' 09.75903"	-84° 15' 33.16621"	155.554
ST_MARYS_14	46° 08' 41.79930"	-84° 05' 55.74831"	146.412
ST_MARYS_15	46° 16' 57.92426"	-84° 12' 56.98723"	148.462
ST_MARYS_16	46° 12' 00.39084"	-84° 03' 07.24829"	145.856
ST_MARYS_17	46° 31' 44.59961"	-84° 35' 04.01988"	149.466
ST_MARYS_18	46° 25' 31.56096"	-84° 05' 16.17047"	141.603
ST_MARYS_19	46° 32' 38.68230"	-84° 08' 05.29663"	157.899
ST_MARYS_RTK_01	45° 57' 07.94064"	-83° 37' 19.91394"	143.807

To correct the continuously recorded onboard measurements of the aircraft position, QSI concurrently conducted multiple static Global Navigation Satellite System (GNSS) ground surveys (1 Hz recording frequency) over each monument. During post-processing, the static GPS data were triangulated with nearby Continuously Operating Reference Stations (CORS) using the Online Positioning User Service (OPUS[1]) for precise positioning. Multiple independent sessions over the same monument were processed to confirm antenna height measurements and to refine position accuracy.

Monuments were established according to the national standard for geodetic control networks, as specified in the Federal Geographic Data Committee (FGDC) Geospatial Positioning Accuracy Standards for geodetic networks.[2] This standard provides guidelines for classification of monument quality at the 95% confidence interval as a basis for comparing the quality of one control network to another. The monument rating for this project is shown in Table 5.

Table 5: Federal Geographic Data Committee monument rating for network accuracy

Direction	Rating
1.96 * St Dev $_{NE}$:	0.020 m
1.96 * St Dev $_{z}$:	0.050 m

[1] OPUS is a free service provided by the National Geodetic Survey to process corrected monument positions. http://www.ngs.noaa.gov/OPUS.

[2] Federal Geographic Data Committee, Geospatial Positioning Accuracy Standards (FGDC-STD-007.2-1998). Part 2: Standards for Geodetic Networks, Table 2.1, page 2-3. http://www.fgdc.gov/standards/projects/FGDC-standards-projects/accuracy/part2/chapter2

For the St. Marys River LiDAR project, the monument coordinates contributed no more than 5.4 cm of positional error to the geolocation of the final ground survey points and LiDAR, with 95% confidence.

Ground Survey Points (GSPs)

Ground survey points were collected using real time kinematic and post-processed kinematic (PPK) survey techniques. A Trimble R6, R7, or R8 base unit was positioned at a nearby monument to broadcast a kinematic correction to a roving Trimble R6 GNSS or a Trimble R8 GNSS receiver. All GSP measurements were made during periods with a Position Dilution of Precision (PDOP) of ≤ 3.0 with at least six satellites in view of the stationary and roving receivers. When collecting RTK and PPK data, the rover records data while stationary for five seconds, then calculates the pseudorange position using at least three one-second epochs. Relative errors for any GSP position must be less than 1.5 cm horizontal and 2.0 cm vertical in order to be accepted. See Table 6 for Trimble unit specifications.

GSPs were collected in areas where good satellite visibility was achieved on paved roads and other hard surfaces such as gravel or packed dirt roads. GSP measurements were not taken on highly reflective surfaces such as center line stripes or lane markings on roads due to the increased noise seen in the laser returns over these surfaces. GSPs were collected within as many flightlines as possible; however the distribution of GSPs depended on ground access constraints and monument locations and may not be equitably distributed throughout the study area (Figure 4).

Table 6: Trimble equipment identification

Receiver Model	Antenna	OPUS Antenna ID	Use
Trimble R6	Integrated GNSS Antenna R6	TRM_R6	Static, Rover
Trimble R7 GNSS	Zephyr GNSS Geodetic Model 2 RoHS	TRM57971.00	Static
Trimble R8	Integrated Antenna R8 Model 2	TRM_R8_GNSS	Static, Rover

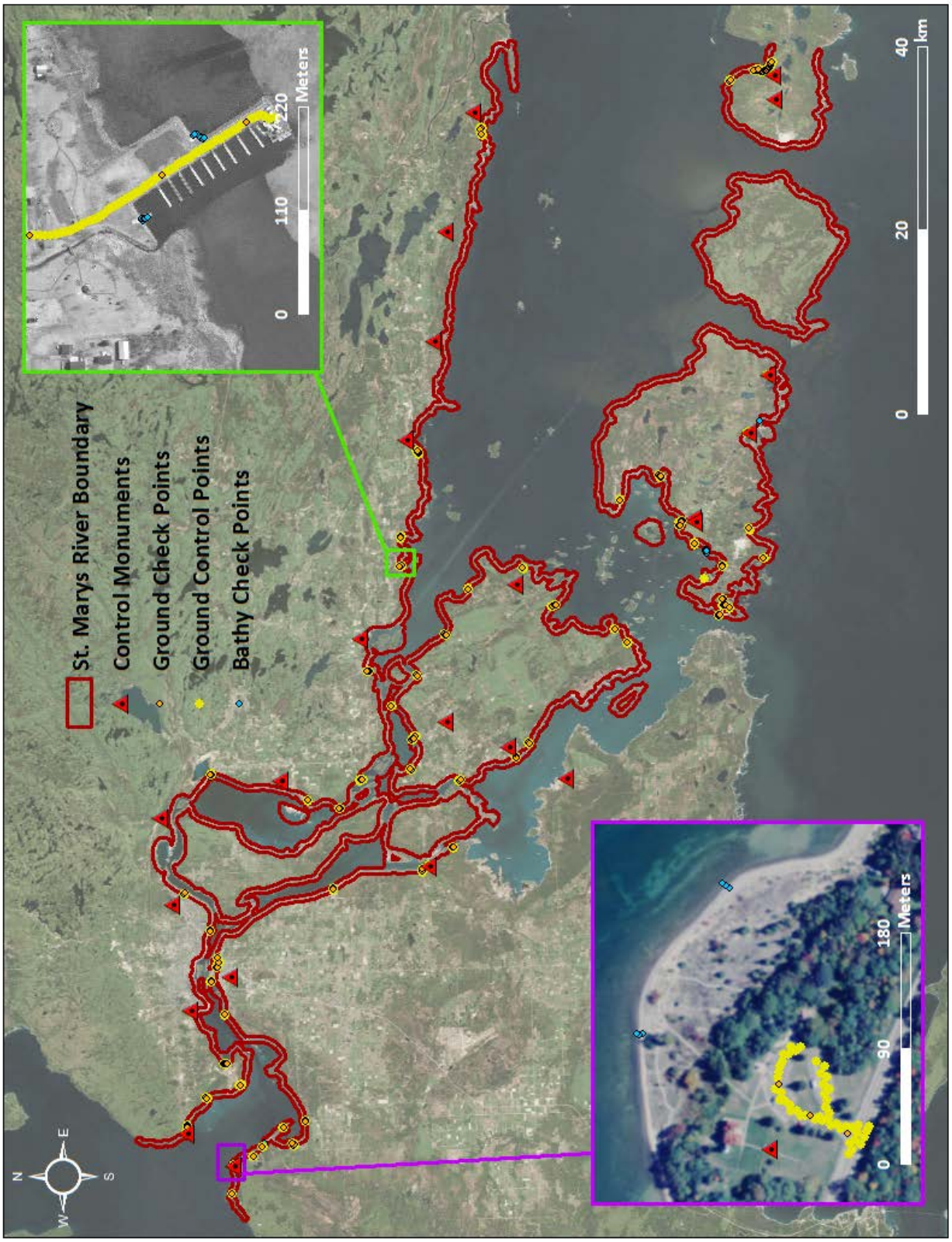

Figure 4: Ground survey location map

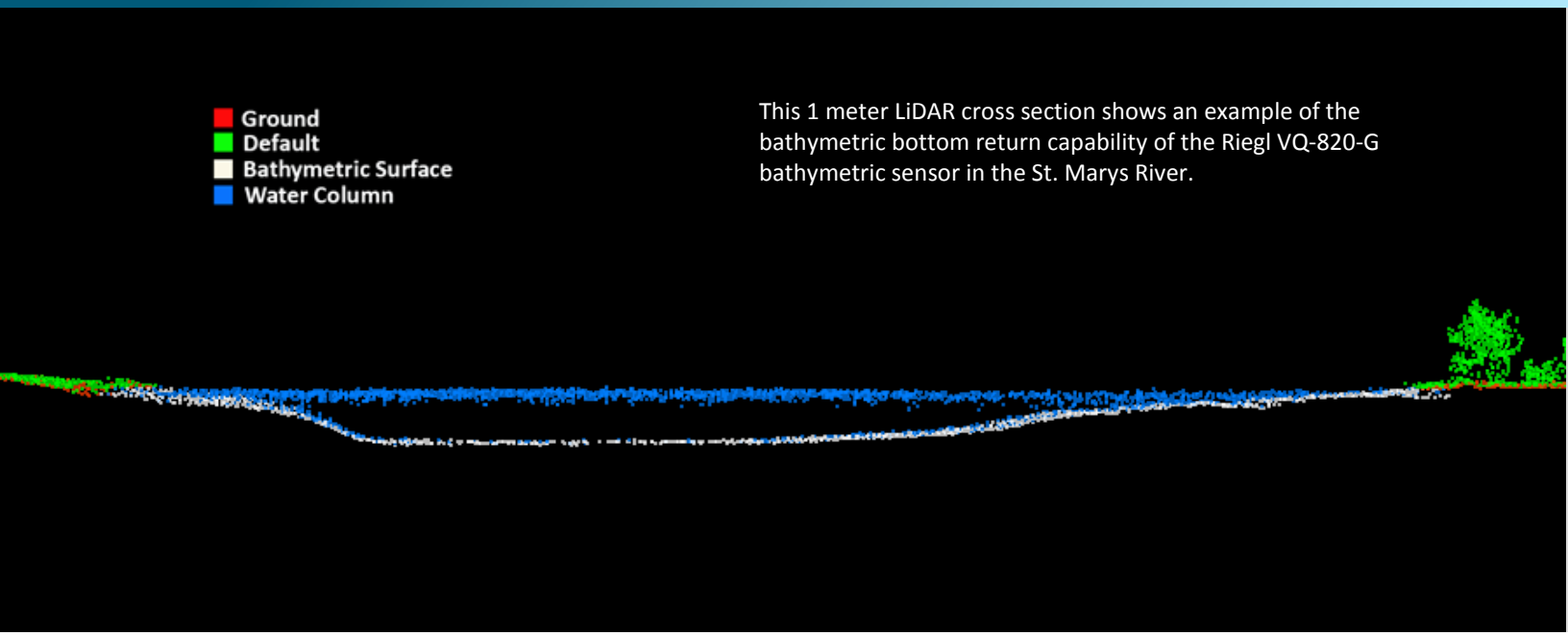

This 1 meter LiDAR cross section shows an example of the bathymetric bottom return capability of the Riegl VQ-820-G bathymetric sensor in the St. Marys River.

Topobathymetric LiDAR Data

Upon completion of data acquisition, QSI processing staff initiated a suite of automated and manual techniques to process the data into the requested deliverables. Processing tasks included GPS control computations, smoothed best estimate trajectory (SBET) calculations, kinematic corrections, calculation of laser point position, sensor and data calibration for optimal relative and absolute accuracy, and LiDAR point classification (Table 7). Riegl's RiProcess software was used to facilitate bathymetric return processing. Once bathymetric points were differentiated, they were spatially corrected for refraction through the water column based on the angle of incidence of the laser. QSI refracted water column points using QSI's proprietary LAS processing software, LAS Monkey. The resulting point cloud data were classified using both manual and automated techniques. Processing methodologies were tailored for the landscape. Brief descriptions of these tasks are shown in Table 8.

Table 7: ASPRS LAS classification standards applied to the St. Marys River dataset

Classification Number	Classification Name	Classification Description
1	Default/Unclassified	Laser returns that are not included in the ground class, composed of vegetation and human-made structures
2	Ground	Laser returns that are determined to be ground using automated and manual cleaning algorithms
7	Noise	Laser returns that are often associated with birds, scattering from reflective surfaces, or artificial points below the ground surface.
9	Water	NIR Laser returns that are determined to be water using automated and manual cleaning algorithms.
13	Submerged Structures	Submerged in-water structures within the Soo Locks footprint (including locks, dams, piers, and gates)
14	Above-Water Structures	Above-water portions of in-water structures within the Soo Locks footprint (including locks, dams, piers, and gates)
25	Water Column	Refracted Riegl sensor returns that are determined to be water using automated and manual cleaning algorithms.
26	Bathymetric Bottom	Refracted Riegl sensor returns that fall within the water's edge breakline which characterize the submerged topography.
29	Submerged Object	Submerged object, not otherwise specified (e.g., wreck, rock, submerged piling)

Table 8: LiDAR processing workflow

LiDAR Processing Step	Software Used
Resolve kinematic corrections for aircraft position data using kinematic aircraft GPS and static ground GPS data. Develop a smoothed best estimate of trajectory (SBET) file that blends post-processed aircraft position with sensor head position and attitude recorded throughout the survey.	Waypoint Inertial Explorer v.8.6 POSPac MMS v6.2
Calculate laser point position by associating SBET position to each laser point return time, scan angle, intensity, etc. Create raw laser point cloud data for the entire survey in *.las (ASPRS v. 1.2) format. Convert data to orthometric elevations by applying a geoid12b correction.	RiProcess v1.6.4 Waypoint Inertial Explorer v.8.6 Leica Cloudpro v. 1.2.1 TerraMatch v.15
Import raw laser points into manageable blocks to perform manual relative accuracy calibration and filter erroneous points. Classify ground points for individual flight lines.	TerraScan v.15
Using ground classified points per each flight line, test the relative accuracy. Perform automated line-to-line calibrations for system attitude parameters (pitch, roll, heading), mirror flex (scale) and GPS/IMU drift. Calculate calibrations on ground classified points from paired flight lines and apply results to all points in a flight line. Use every flight line for relative accuracy calibration.	TerraMatch v.15 RiProcess v1.6.4
Apply refraction correction to all subsurface returns.	LAS Monkey 2.1 (QSI Proprietary)
Classify resulting data to ground and other client designated ASPRS classifications (Table 7). Assess statistical absolute accuracy via direct comparisons of ground classified points to ground control survey data.	TerraScan v.16 TerraModeler v.16
Generate bare earth models as triangulated surfaces. Generate highest hit models as a surface expression of all classified points. Export all surface models as ESRI GRIDs at a 1 meter pixel resolution.	TerraScan v.16 TerraModeler v.16 ArcMap v. 10.1
Export intensity images as GeoTIFFs at a 0.5 meter pixel resolution.	TerraScan v.16 TerraModeler v.16 Las Product Creator (QSI Proprietary) ArcMap v. 10.1

Bathymetric Refraction

The water surface model used for refraction is generated using NIR points within the breaklines defining the water's edge. Points are filtered and edited to obtain the most accurate representation of the water surface and are used to create a water surface model TIN. A tin model is preferable to a raster based water surface model to obtain the most accurate angle of incidence during refraction. The refraction processing is done using Las Monkey; QSI's proprietary LiDAR processing tool. After refraction, the points are compared against bathymetric control points to assess accuracy.

LiDAR Derived Products

Because hydrographic laser scanners penetrate the water surface to map submerged topography, this affects how the data should be processed and presented in derived products from the LiDAR point cloud. The following discusses certain derived products that vary from the traditional (NIR) specification and delivery format.

Topobathymetric DEMs

Bathymetric bottom returns can be limited by depth, water clarity, and bottom surface reflectivity. Water clarity and turbidity affects the depth penetration capability of the green wavelength laser with returning laser energy diminishing by scattering throughout the water column. Additionally, the bottom surface must be reflective enough to return remaining laser energy back to the sensor at a detectable level. Although the predicted depth penetration range of the Riegl VQ-820-G sensor is one Secchi depth on brightly reflective surfaces, it is not unexpected to have no bathymetric bottom returns in turbid or non-reflective areas.

As a result, creating digital elevation models (DEMs) presents a challenge with respect to interpolation of areas with no returns. Traditional DEMs are "unclipped", meaning areas lacking ground returns are interpolated from neighboring ground returns (or breaklines in the case of hydro-flattening), with the assumption that the interpolation is close to reality. In bathymetric modeling, these assumptions are prone to error because a lack of bathymetric returns can indicate a change in elevation that the laser can no longer map due to increased depths. The resulting void areas may suggest greater depths, rather than similar elevations from neighboring bathymetric bottom returns. Therefore, QSI analyzed these areas and created a shape to show areas where the bathymetry was unable to be mapped due to increased depth, lower surface reflectivity, or water turbidity. This shapefile was used to control the extent of the delivered clipped topobathymetric model to avoid false triangulation (interpolation from TIN'ing) across areas in the water with no bathymetric returns.

Intensity Images

Due to the different wavelengths between the NIR and Green LiDAR sensors, combining intensity information into one image can result in muddled or streaky images difficult to analyze despite both intensity values being in the 16-bit range. Therefore, NIR and Green returns were split into different datasets to provide clearer intensity images for each sensor (Figure 5).

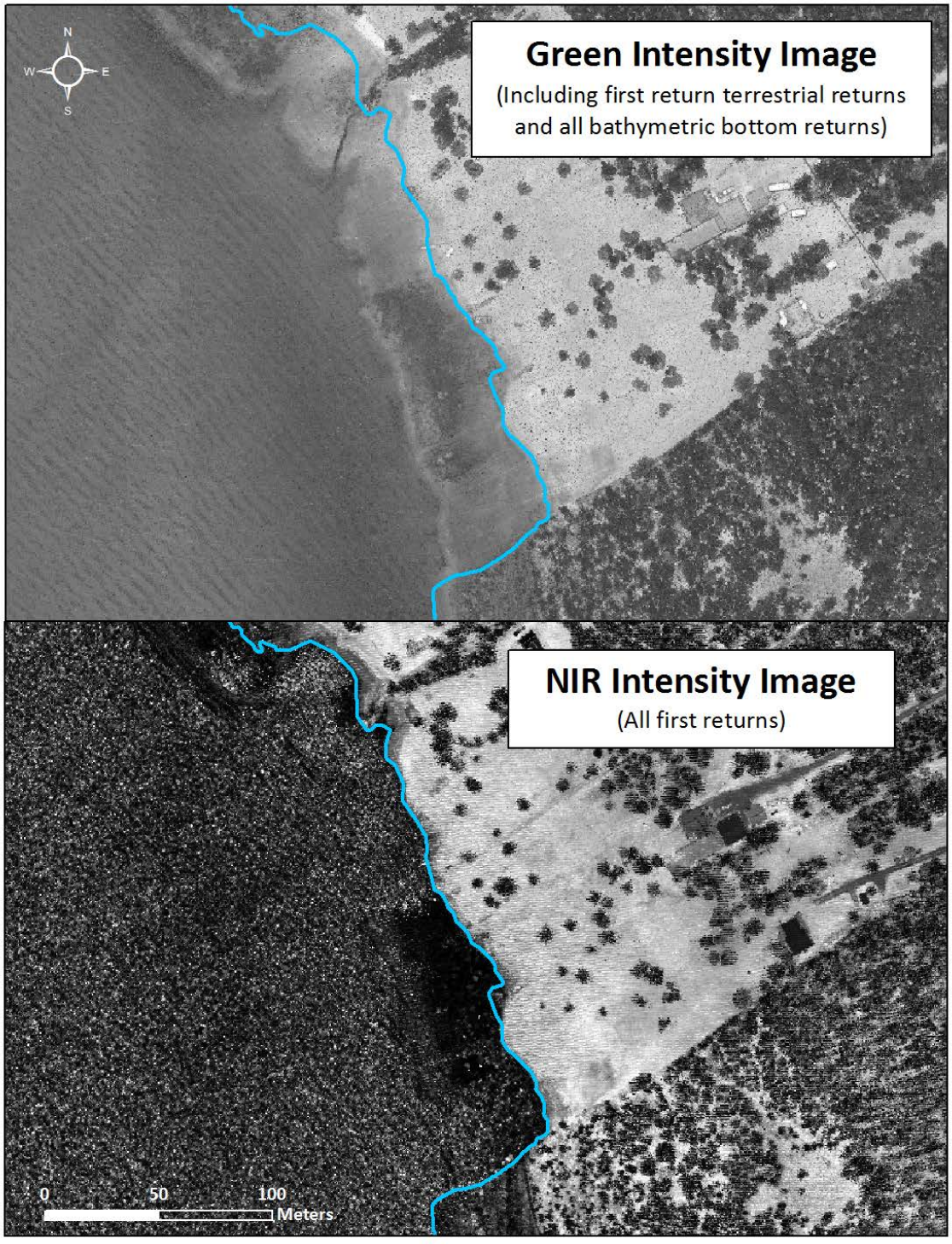

Figure 5: A sample image from the St. Marys River project area showing the comparison of Intensity Images from Green and NIR returns

Feature Extraction

Contours

Contour generation from LiDAR point data required a thinning operation in order to reduce contour sinuosity. The thinning operation reduced point density where topographic change is minimal (i.e., flat surfaces) while preserving resolution where topographic change was present. Model key points were selected from the ground and bathymetric classified points. Generation of model key points eliminated redundant detail in terrain representation, particularly in areas of low relief, and provided for a more manageable dataset. Contours were produced through TerraModeler by interpolating between the model key points at even elevation increments.

Elevation contour lines were clipped to the extent of good bathymetric coverage and then intersected with the bathymetric void shape. Contours which crossed areas of voids were classified as low confidence, while all other contours are classified as high confidence (Figure 6).

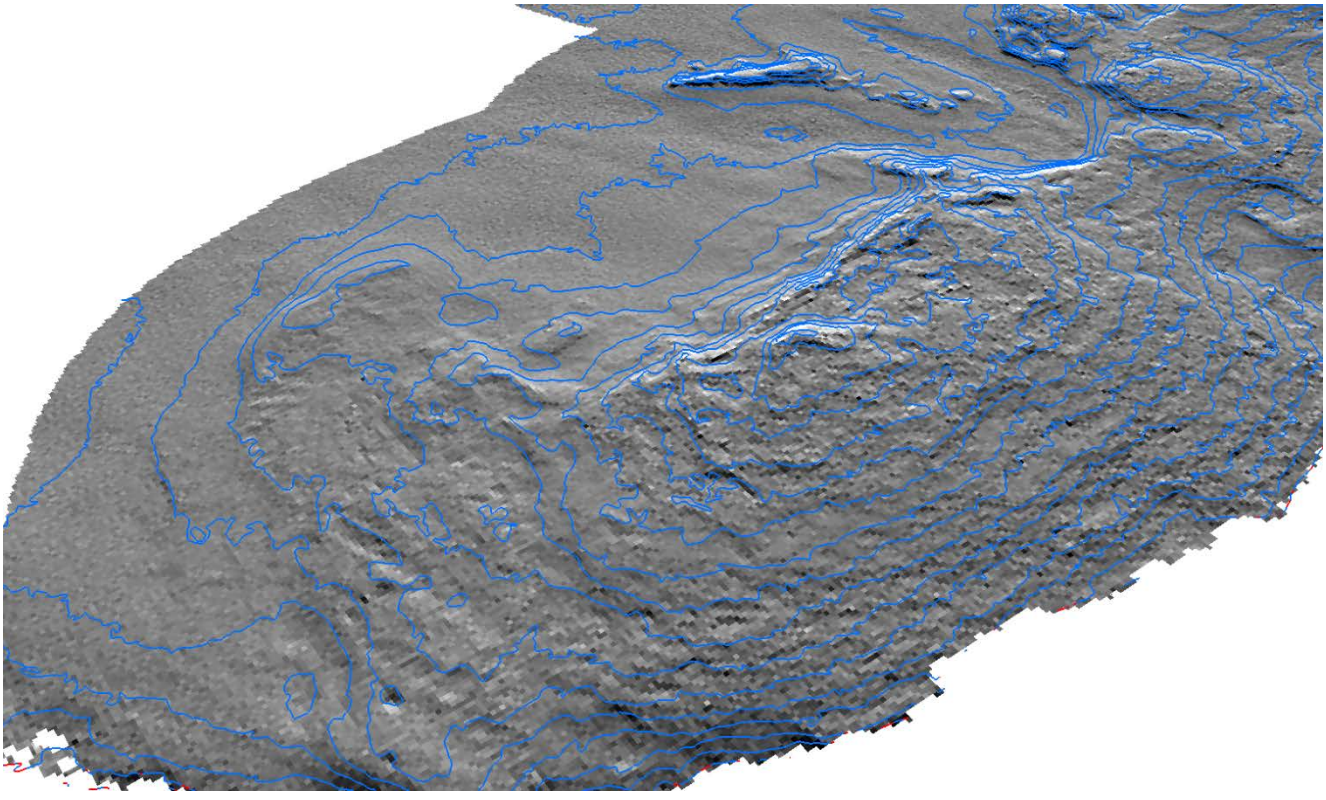

Figure 6: Contours draped over the St. Marys River bare earth elevation model. Blue contours represent high confidence while the red contours represent low confidence.

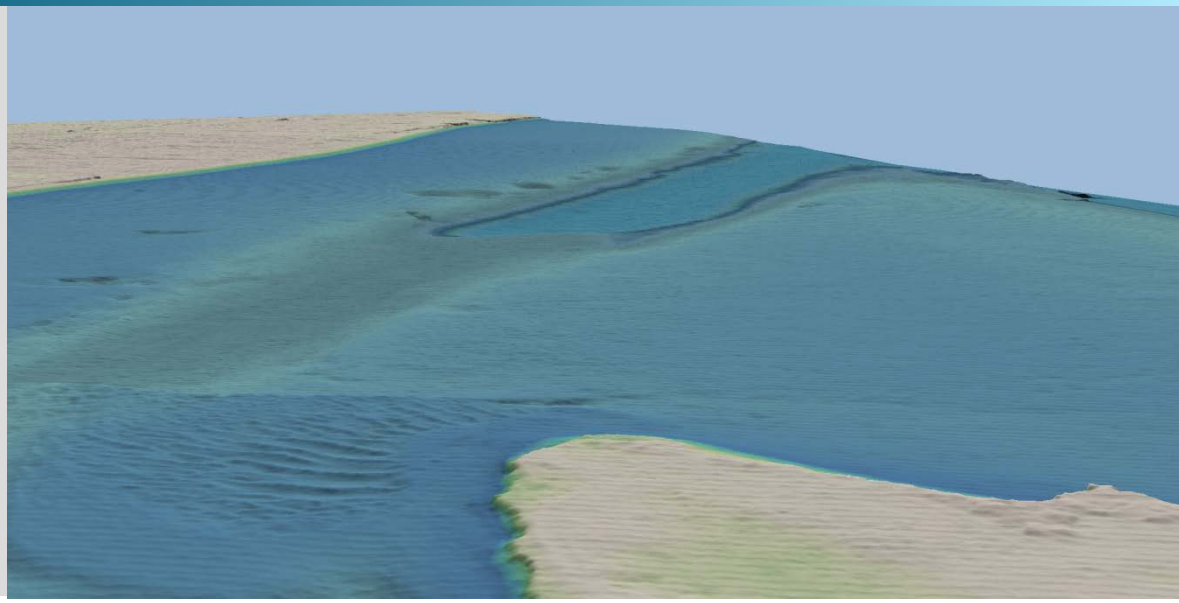

This image displays the submerged topography of the St. Marys River bottom near Pointe-Louise. The image was created from the gridded LiDAR surface colored by elevation.

Bathymetric LiDAR

An underlying principle for collecting hydrographic LiDAR data is to survey near-shore areas that can be difficult to collect with other methods, such as multi-beam sonar, particularly over large areas. In order to determine the capability and effectiveness of the bathymetric LiDAR, bathymetric return density and spatial accuracy were considered.

Mapped Bathymetry

The specified depth penetration range of the Riegl VQ-820-G sensor is one secchi depth; therefore, bathymetry data below one secchi depth at the time of acquisition is not to be expected. To assist in evaluating performance results of the sensor, a polygon layer was created to delineate areas where bathymetry was successfully mapped.

This shapefile was used to control the extent of the delivered clipped topo-bathymetric model and to avoid false triangulation across areas in the water with no returns. Insufficiently mapped areas were identified by triangulating bathymetric bottom points with an edge length maximum of 4.56 meters. This ensured all areas of no returns (> 9 m^2), were identified as data voids.

LiDAR Point Density

First Return Point Density

The acquisition parameters were designed to acquire an average first-return density of 4 points/m^2 for the topo-bathymetric AOI, and 6 points/ m^2 for the NIR AOI. First return density describes the density of pulses emitted from the laser that return at least one echo to the system. Multiple returns from a single pulse were not considered in first return density analysis. Some types of surfaces (e.g., breaks in terrain, water and steep slopes) may have returned fewer pulses than originally emitted by the laser.

With NIR LiDAR, first returns typically reflect off the highest feature on the landscape within the footprint of the pulse. In forested or urban areas the highest feature could be a tree, building or power line, while in areas of unobstructed ground, the first return will be the only echo and represents the bare earth surface. With Bathymetric, or Green LiDAR, the first return will represent water surface or water column returns.

The average first-return density of the green wavelength LiDAR data for the St. Marys River project was 15.79 points/m^2 while the average first-return density of the NIR wavelength LiDAR data was 16.63 m^2. The cumulative first return density average from all sensors was 28.23 points/m^2. The statistical and spatial distributions of all first return densities per 100 m x 100 m cell are portrayed in Figure 7 through Figure 12.

Table 9: Average First Return LiDAR point densities

First Return Type	Point Density
Green Sensor First Returns	15.79 points/m^2
NIR Sensor First Returns	16.63 points/m^2
Topobathy AOI Cumulative First Returns	28.23 points/m^2

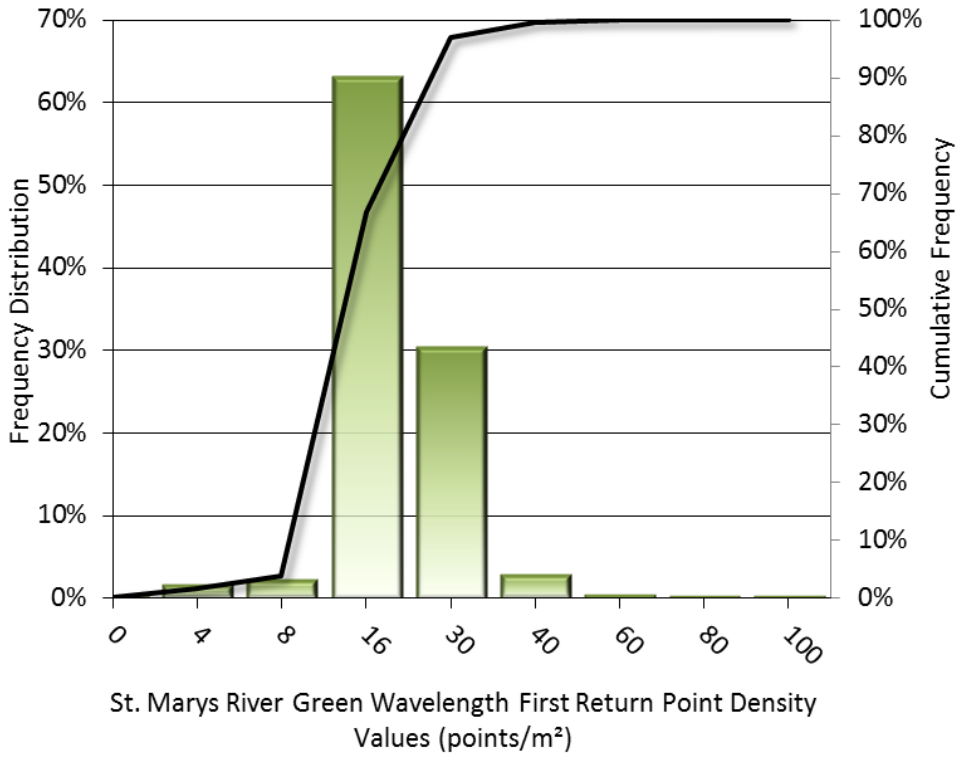

Figure 7: Frequency distribution of green sensor first return densities per 100 x 100 m cell

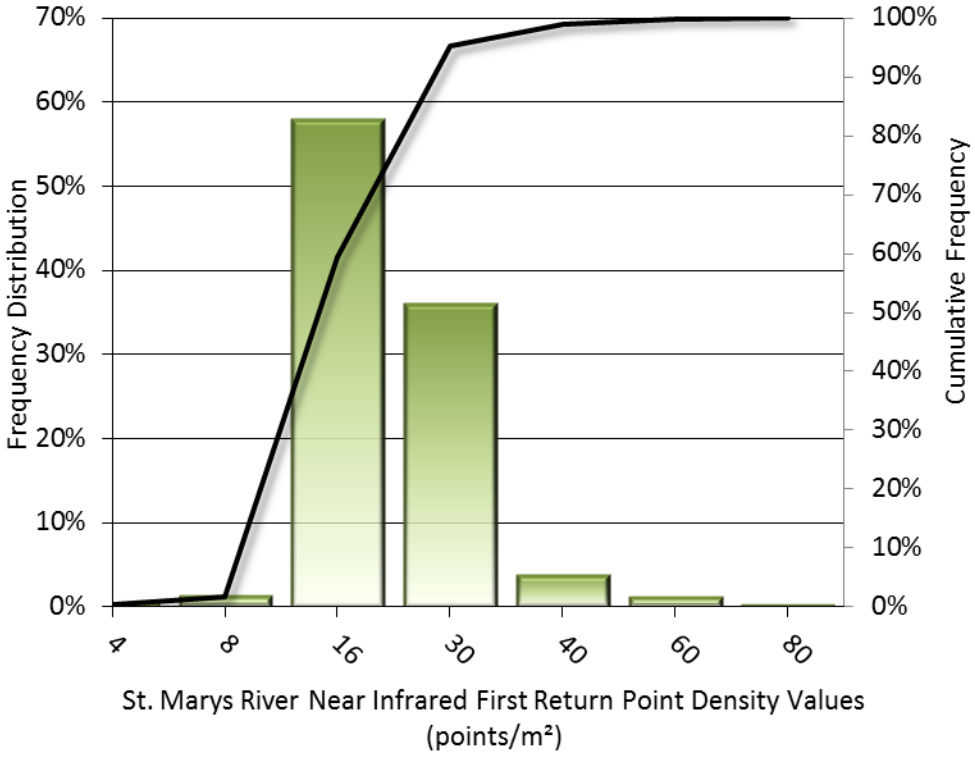

Figure 8: Frequency distribution of NIR first return densities per 100 x 100 m cell

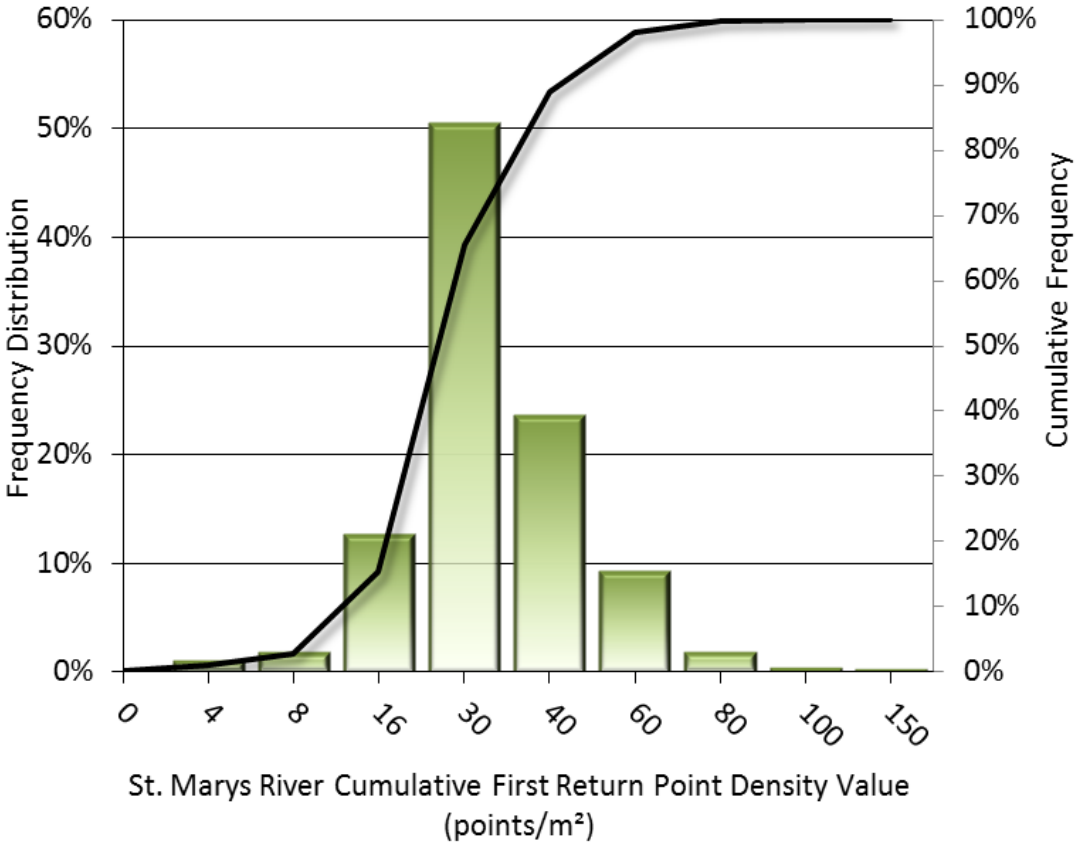

Figure 9: Frequency distribution of cumulative first return densities per 100 x 100 m cell

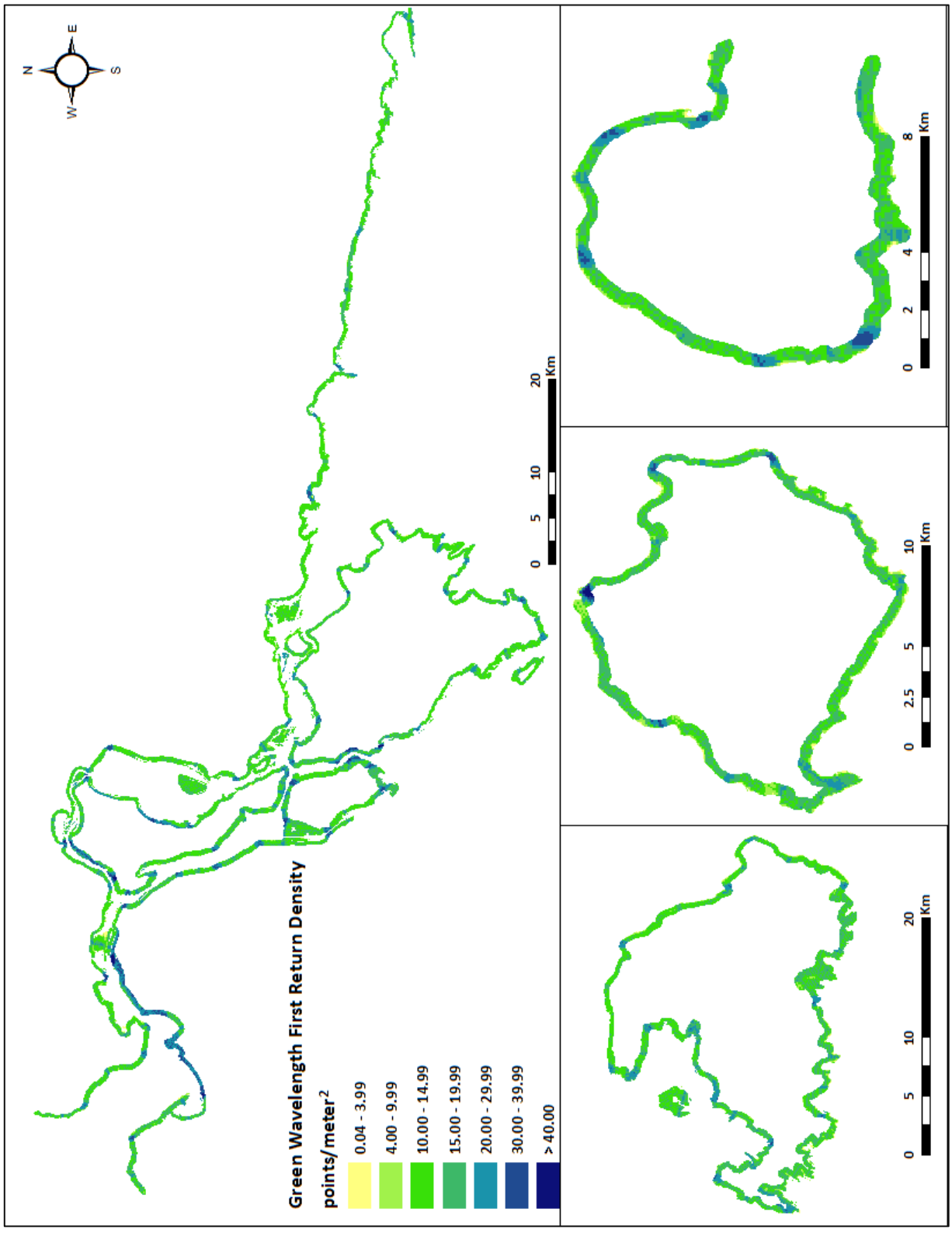

Figure 10: Green first return density map for the St. Marys River site (100 m x 100 m cells)

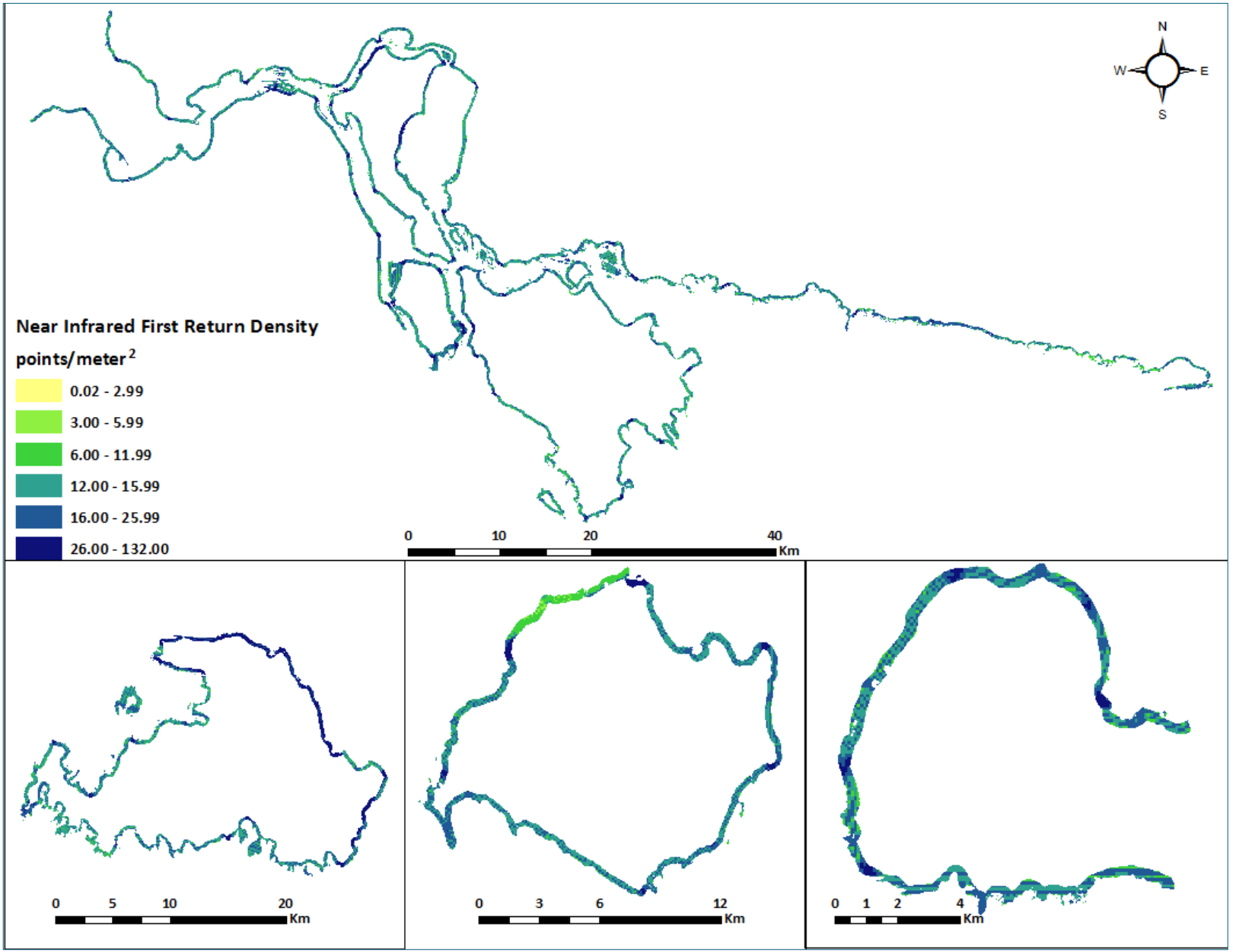

Figure 11: NIR first return density map for the St. Marys River site (100 m x 100 m cells)

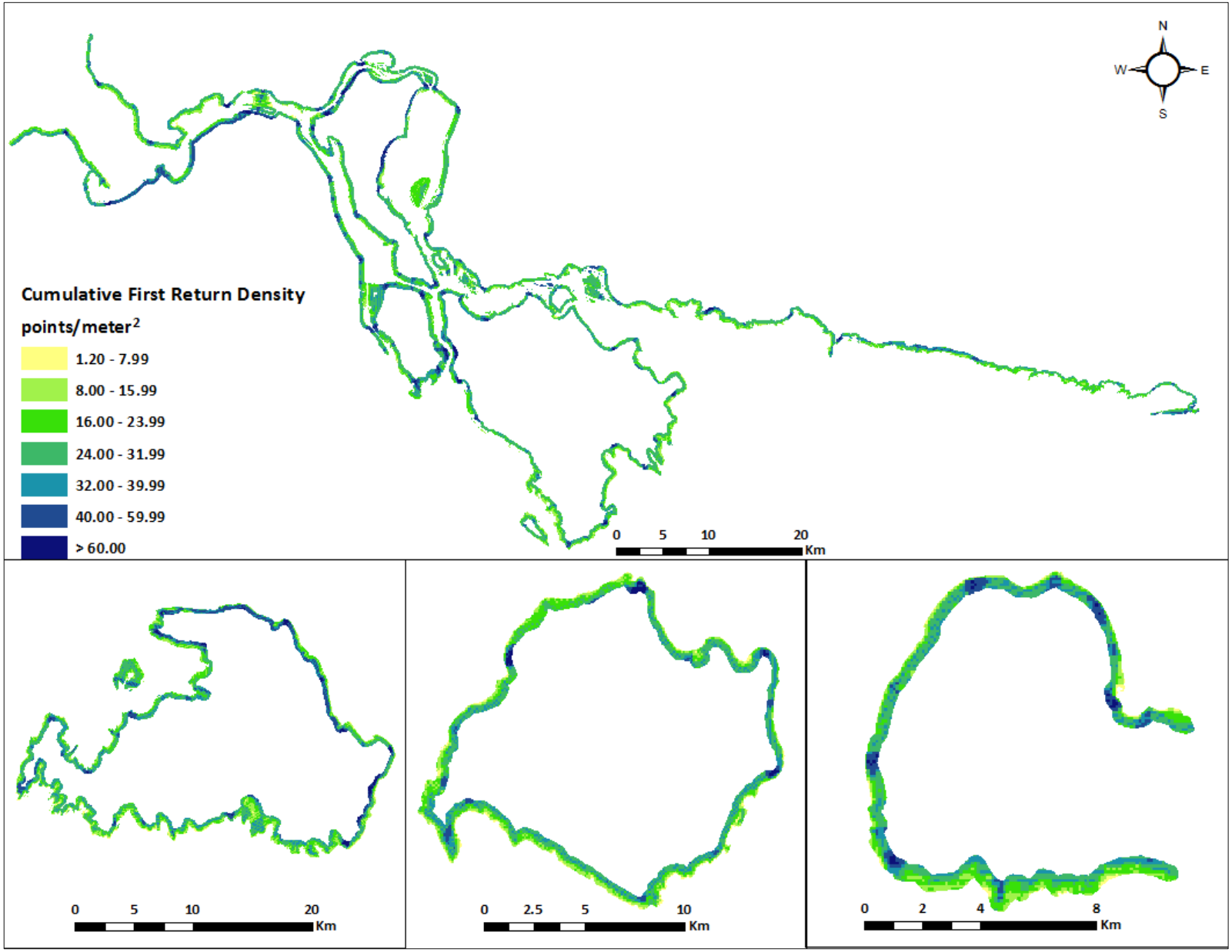

Figure 12: Cumulative first return density map for the St. Marys River site (100 m x 100 m cells)

Bathymetric and Ground Classified Point Densities

The density of ground classified LiDAR returns and bathymetric bottom returns were also analyzed for this project. Terrain character, land cover, and ground surface reflectivity all influenced the density of ground and bathymetric surface returns. In vegetated areas, fewer pulses may have penetrated the canopy, resulting in lower ground density. Similarly, the density of bathymetric bottom returns was influenced by turbidity, depth, and bottom surface reflectivity. In turbid areas, fewer pulses may have penetrated the water surface, resulting in lower bathymetric density.

The ground and bathymetric bottom classified density of LiDAR data for the St. Marys River project was 6.83 points/m^2. The statistical and spatial distributions ground classified and bathymetric bottom return densities per 100 m x 100 m cell are portrayed in Figure 13 and Figure 14.

Table 10: Average Ground and Bathymetric Classified LiDAR point densities

Classification	Point Density
Ground and Bathymetric Bottom Classified Returns	6.83 points/m^2

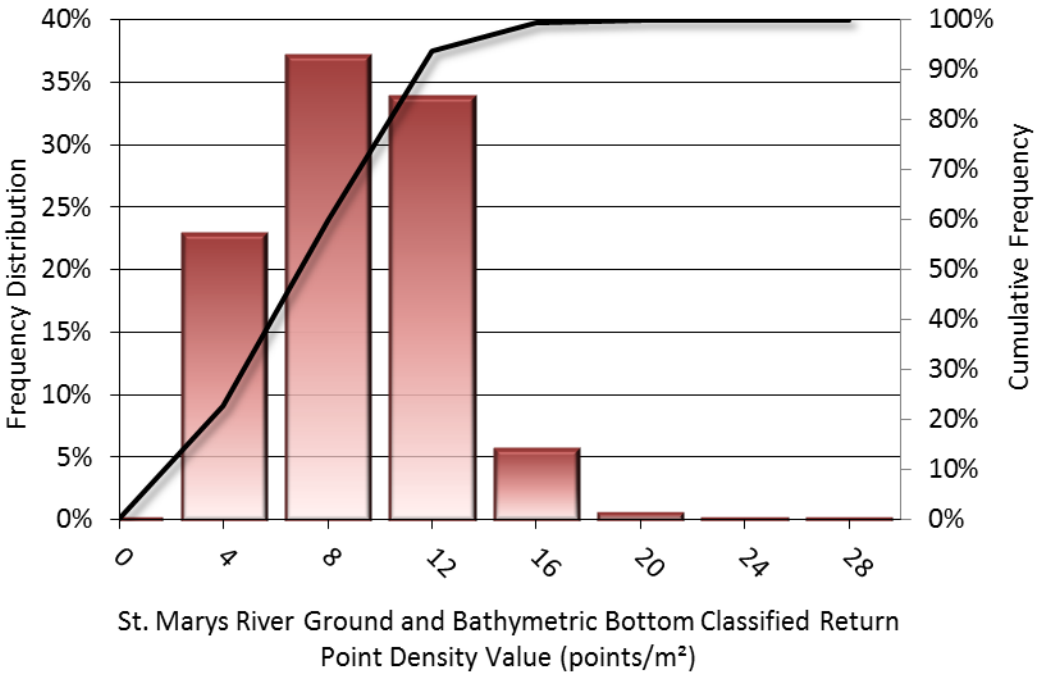

Figure 13: Frequency distribution of ground return densities per 100 x 100 m cell

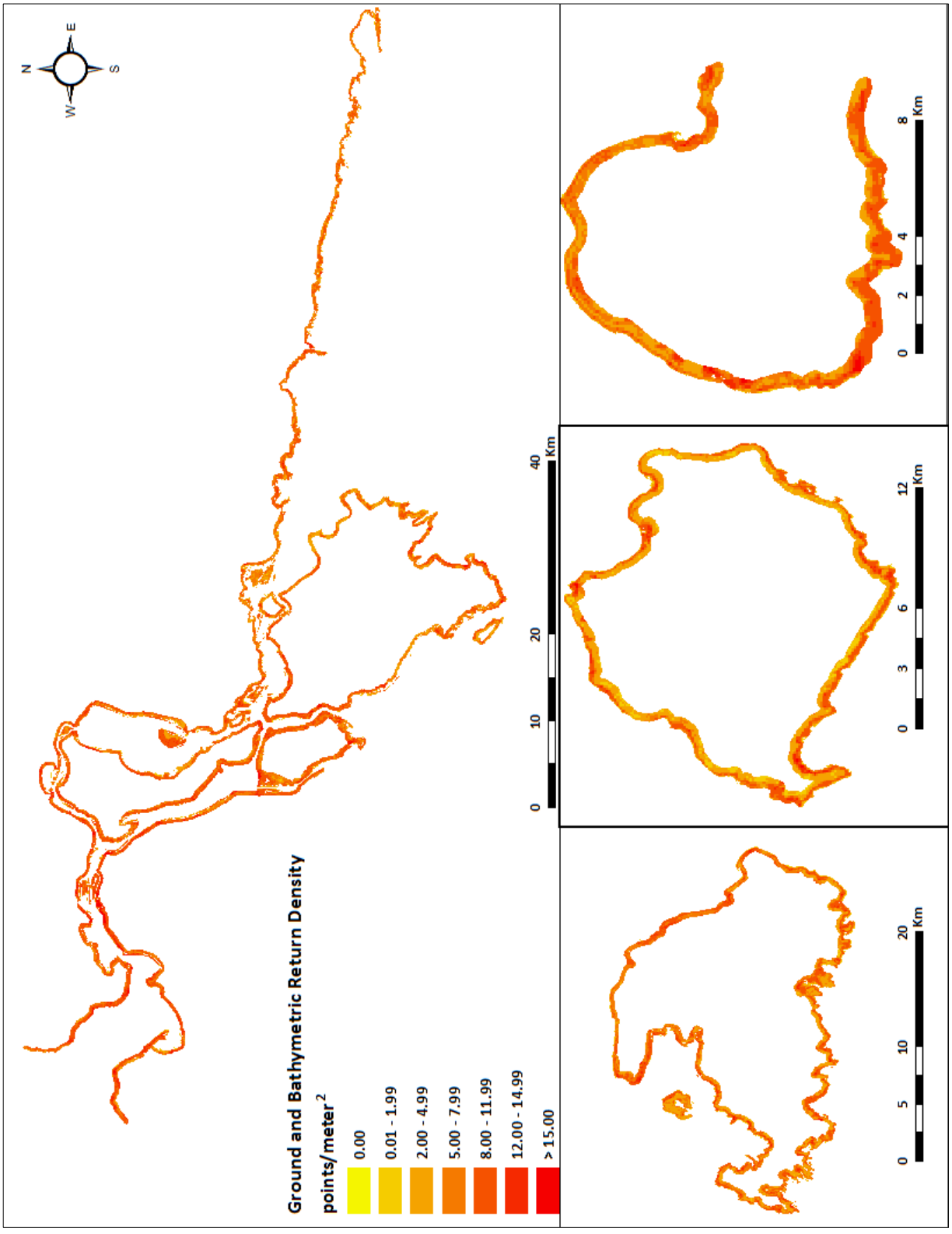

Figure 14: Ground and Bathymetric Bottom classified density map for the St. Marys River site (100 m x 100 m cells)

LiDAR Accuracy Assessments

The accuracy of the LiDAR data collection can be described in terms of absolute accuracy (the consistency of the data with external data sources) and relative accuracy (the consistency of the dataset with itself). See Appendix A for further information on sources of error and operational measures used to improve relative accuracy.

LiDAR Absolute Accuracy

Absolute accuracy was assessed using Fundamental Vertical Accuracy (FVA) reporting designed to meet guidelines presented in the FGDC National Standard for Spatial Data Accuracy[3]. FVA compares known ground check point data collected on open, bare earth surfaces with level slope (<20°) to the triangulated surface generated by the LiDAR points. FVA is a measure of the accuracy of LiDAR point data in open areas where the LiDAR system has a high probability of measuring the ground surface and is evaluated at the 95% confidence interval (1.96 * RMSE), as shown in Table 11.

The mean and standard deviation (sigma σ) of divergence of the ground surface model from ground check point coordinates are also considered during accuracy assessment. These statistics assume the error for x, y and z is normally distributed, and therefore the skew and kurtosis of distributions are also considered when evaluating error statistics. For the St. Marys River survey, 164 ground check points were withheld in total resulting in a fundamental vertical accuracy of 0.045 meters (Figure 15).

Additionally, 334 bathymetric (submerged or along the water's edge) check points were also collected in order to assess the submerged surface vertical accuracy, resulting in an average accuracy of -0.013 meters.

QSI also assessed absolute accuracy using 3,092 ground control points. Although these points were used in the calibration and post-processing of the LiDAR point cloud, they may still provide a good indication of the overall accuracy of the LiDAR dataset, and therefore have been provided in below.

Table 11: Absolute accuracy results

Absolute Accuracy			
	Ground Check Points (FVA)	**Bathymetric Check Points**	**Ground Control Points**
Sample	164 points	334 points	3092 points
FVA (1.96*RMSE)	0.045 m	0.094 m	0.047 m
Average	-0.007 m	-0.013 m	-0.010 m
Median	-0.007 m	-0.019 m	-0.009 m
RMSE	0.023 m	0.048 m	0.024 m
Standard Deviation (1σ)	0.022 m	0.046 m	0.022 m

[3] Federal Geographic Data Committee, Geospatial Positioning Accuracy Standards (FGDC-STD-007.3-1998). Part 3: National Standard for Spatial Data Accuracy. http://www.fgdc.gov/standards/projects/FGDC-standards-projects/accuracy/part3/chapter3

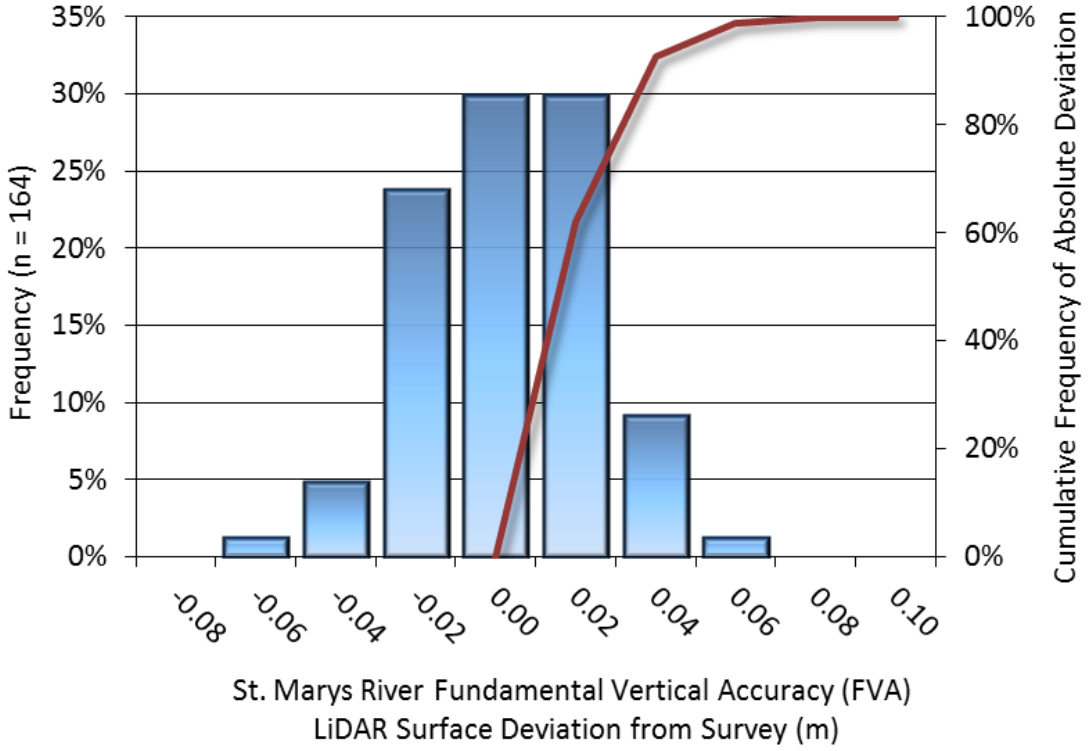

Figure 15: Frequency histogram for LiDAR surface deviation from ground check point values

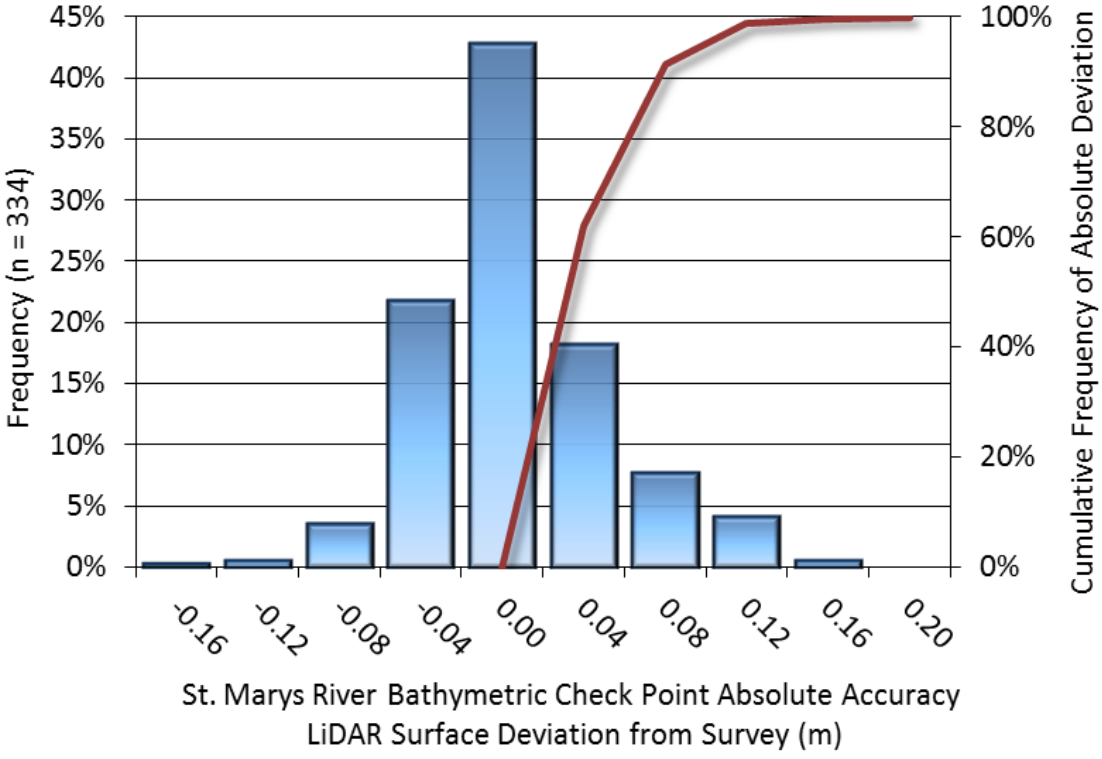

Figure 16: Frequency histogram for LiDAR surface deviation from bathymetric check point values

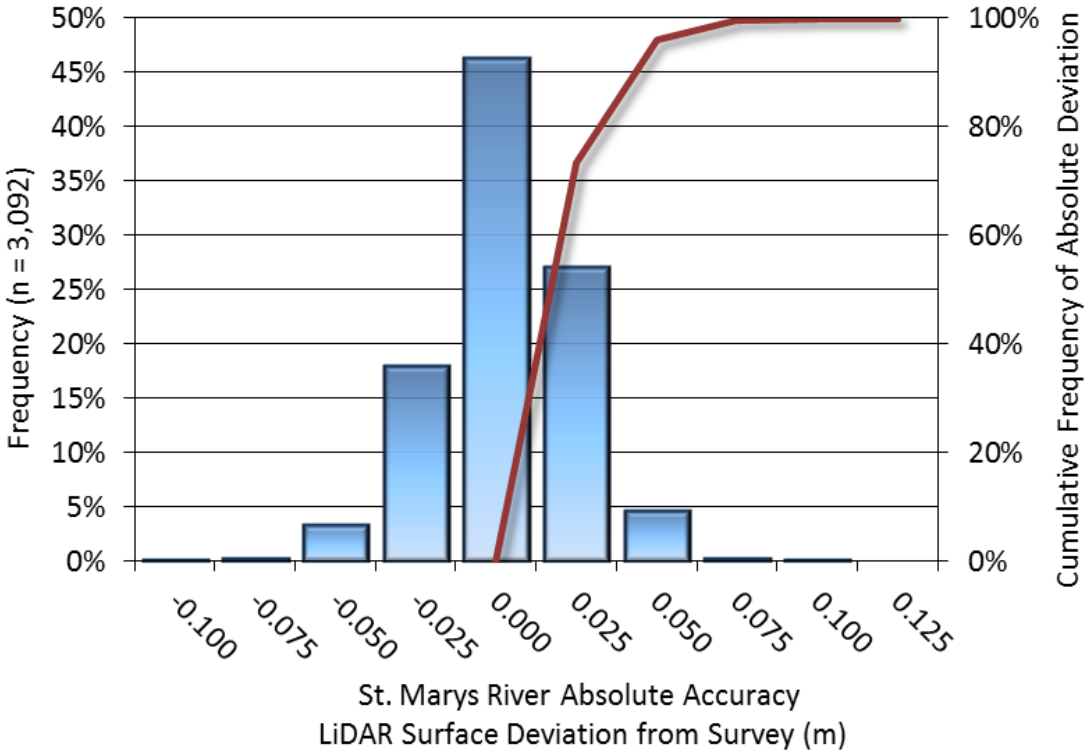

Figure 17: Frequency histogram for LiDAR surface deviation from ground control point values

LiDAR Relative Vertical Accuracy

Relative vertical accuracy refers to the internal consistency of the data set as a whole: the ability to place an object in the same location given multiple flight lines, GPS conditions, and aircraft attitudes. When the LiDAR system is well calibrated, the swath-to-swath vertical divergence is low (<0.10 meters). The relative vertical accuracy was computed by comparing the ground surface model of each individual flight line with its neighbors in overlapping regions. The average (mean) line to line relative vertical accuracy for the St. Marys River LiDAR project was 0.029 meters (Table 12, Figure 18).

Table 12: Relative accuracy results

Relative Accuracy	
Sample	2,464 surfaces
Average	0.035 m
Median	0.029 m
RMSE	0.033 m
Standard Deviation (1σ)	0.012 m
1.96σ	0.024m

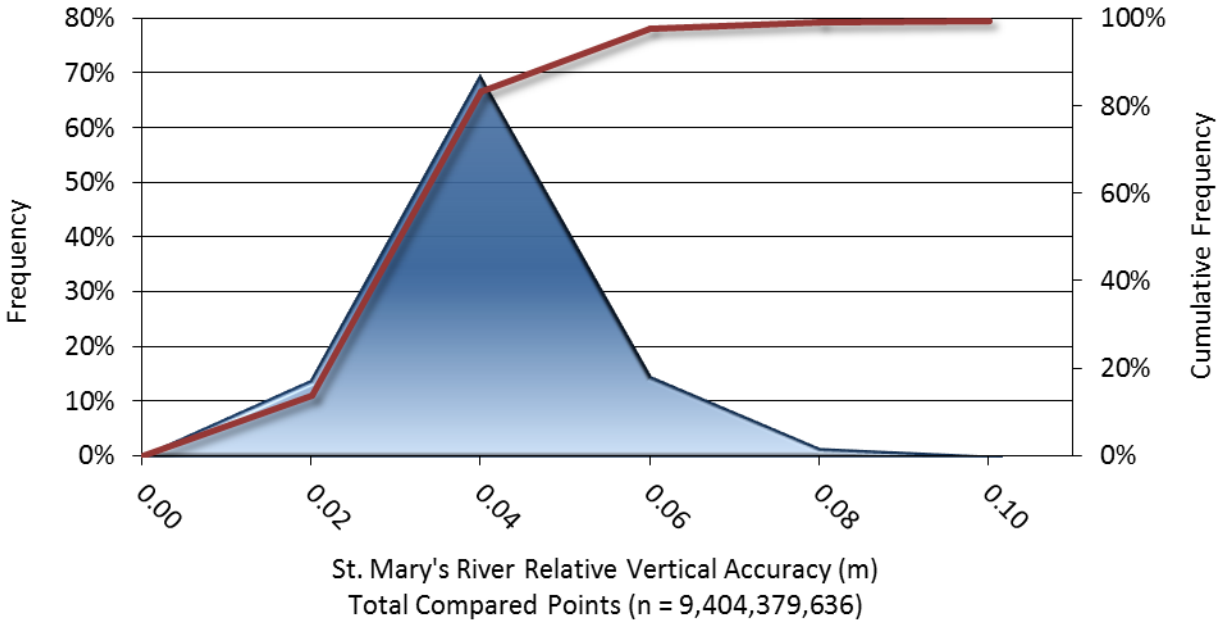

Figure 18: Frequency plot for relative vertical accuracy between flight lines

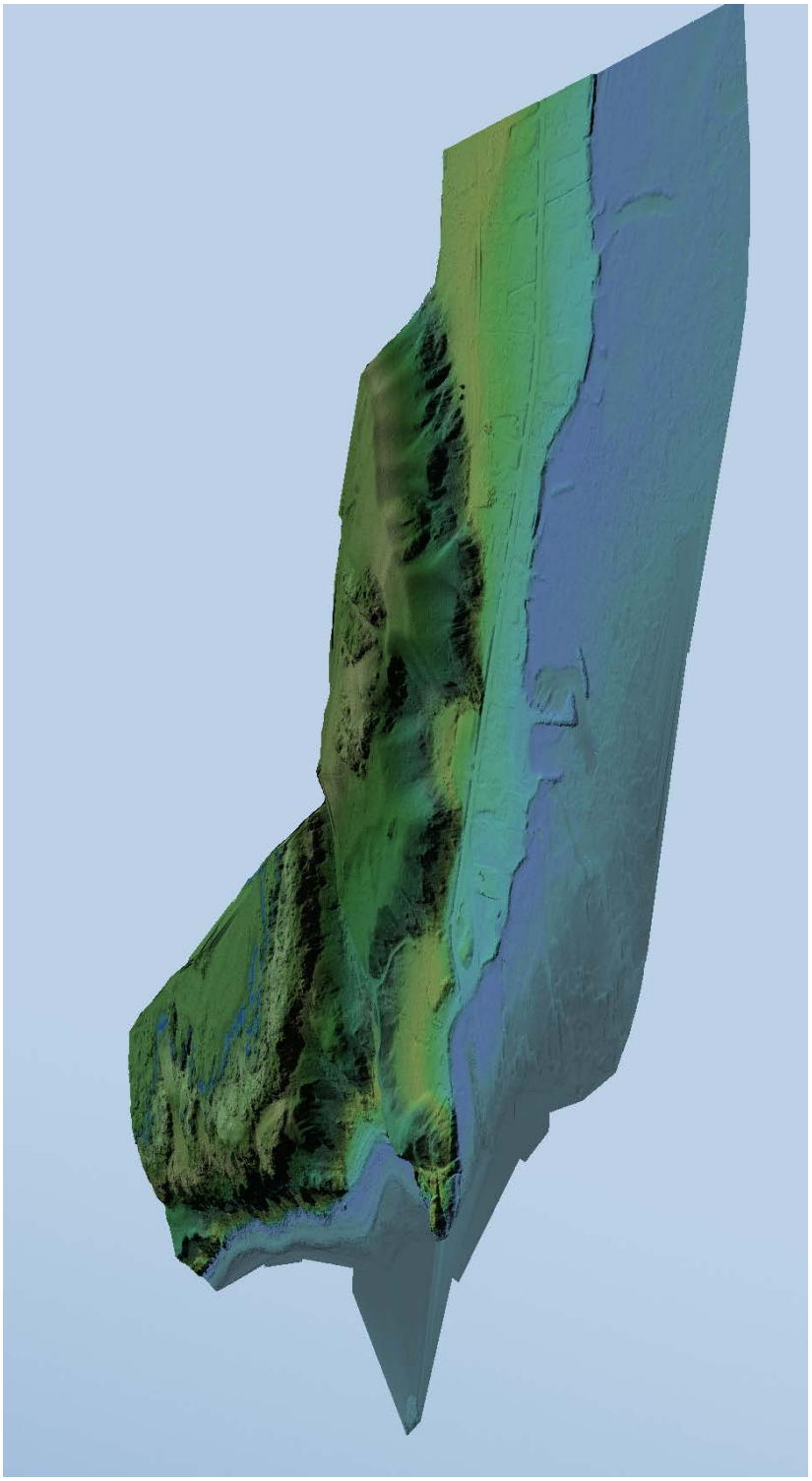

Figure 19: A view looking North at Gros Cap Conservation Area and Lake Superior. The image was created from the LiDAR bare earth model colored by elevation.

GLOSSARY

1-sigma (σ) Absolute Deviation: Value for which the data are within one standard deviation (approximately 68th percentile) of a normally distributed data set.

1.96 * RMSE Absolute Deviation: Value for which the data are within two standard deviations (approximately 95th percentile) of a normally distributed data set, based on the FGDC standards for Fundamental Vertical Accuracy (FVA) reporting.

Accuracy: The statistical comparison between known (surveyed) points and laser points. Typically measured as the standard deviation (sigma σ) and root mean square error (RMSE).

> **Absolute Accuracy:** The vertical accuracy of LiDAR data is described as the mean and standard deviation (sigma σ) of divergence of LiDAR point coordinates from ground survey point coordinates. To provide a sense of the model predictive power of the dataset, the root mean square error (RMSE) for vertical accuracy is also provided. These statistics assume the error distributions for x, y and z are normally distributed, and thus we also consider the skew and kurtosis of distributions when evaluating error statistics.
>
> **Relative Accuracy:** Relative accuracy refers to the internal consistency of the data set; i.e., the ability to place a laser point in the same location over multiple flight lines, GPS conditions and aircraft attitudes. Affected by system attitude offsets, scale and GPS/IMU drift, internal consistency is measured as the divergence between points from different flight lines within an overlapping area. Divergence is most apparent when flight lines are opposing. When the LiDAR system is well calibrated, the line-to-line divergence is low (<10 cm).
>
> **Root Mean Square Error (RMSE):** A statistic used to approximate the difference between real-world points and the LiDAR points. It is calculated by squaring all the values, then taking the average of the squares and taking the square root of the average.

Data Density: A common measure of LiDAR resolution, measured as points per square meter.

Digital Elevation Model (DEM): File or database made from surveyed points, containing elevation points over a contiguous area. Digital terrain models (DTM) and digital surface models (DSM) are types of DEMs. DTMs consist solely of the bare earth surface (ground points), while DSMs include information about all surfaces, including vegetation and man-made structures.

Intensity Values: The peak power ratio of the laser return to the emitted laser, calculated as a function of surface reflectivity.

Nadir: A single point or locus of points on the surface of the earth directly below a sensor as it progresses along its flight line.

Overlap: The area shared between flight lines, typically measured in percent. 100% overlap is essential to ensure complete coverage and reduce laser shadows.

Pulse Rate (PR): The rate at which laser pulses are emitted from the sensor; typically measured in thousands of pulses per second (kHz).

Pulse Returns: For every laser pulse emitted, the number of wave forms (i.e., echos) reflected back to the sensor. Portions of the wave form that return first are the highest element in multi-tiered surfaces such as vegetation. Portions of the wave form that return last are the lowest element in multi-tiered surfaces.

Real-Time Kinematic (RTK) Survey: A type of surveying conducted with a GPS base station deployed over a known monument with a radio connection to a GPS rover. Both the base station and rover receive differential GPS data and the baseline correction is solved between the two. This type of ground survey is accurate to 1.5 cm or less.

Post-Processed Kinematic (PPK) Survey: GPS surveying is conducted with a GPS rover collecting concurrently with a GPS base station set up over a known monument. Differential corrections and precisions for the GNSS baselines are computed and applied after the fact during processing. This type of ground survey is accurate to 1.5 cm or less.

Scan Angle: The angle from nadir to the edge of the scan, measured in degrees. Laser point accuracy typically decreases as scan angles increase.

Native LiDAR Density: The number of pulses emitted by the LiDAR system, commonly expressed as pulses per square meter.

Relative Accuracy Calibration Methodology:

Manual System Calibration: Calibration procedures for each mission require solving geometric relationships that relate measured swath-to-swath deviations to misalignments of system attitude parameters. Corrected scale, pitch, roll and heading offsets were calculated and applied to resolve misalignments. The raw divergence between lines was computed after the manual calibration was completed and reported for each survey area.

Automated Attitude Calibration: All data were tested and calibrated using TerraMatch automated sampling routines. Ground points were classified for each individual flight line and used for line-to-line testing. System misalignment offsets (pitch, roll and heading) and scale were solved for each individual mission and applied to respective mission datasets. The data from each mission were then blended when imported together to form the entire area of interest.

Automated Z Calibration: Ground points per line were used to calculate the vertical divergence between lines caused by vertical GPS drift. Automated Z calibration was the final step employed for relative accuracy calibration.

LiDAR accuracy error sources and solutions:

Type of Error	Source	Post Processing Solution
GPS (Static/Kinematic)	Long Base Lines	None
	Poor Satellite Constellation	None
	Poor Antenna Visibility	Reduce Visibility Mask
Relative Accuracy	Poor System Calibration	Recalibrate IMU and sensor offsets/settings
	Inaccurate System	None
Laser Noise	Poor Laser Timing	None
	Poor Laser Reception	None
	Poor Laser Power	None
	Irregular Laser Shape	None

Operational measures taken to improve relative accuracy:

Low Flight Altitude: Terrain following was employed to maintain a constant above ground level (AGL). Laser horizontal errors are a function of flight altitude above ground (about 1/3000th AGL flight altitude).

Focus Laser Power at narrow beam footprint: A laser return must be received by the system above a power threshold to accurately record a measurement. The strength of the laser return (i.e., intensity) is a function of laser emission power, laser footprint, flight altitude and the reflectivity of the target. While surface reflectivity cannot be controlled, laser power can be increased and low flight altitudes can be maintained.

Reduced Scan Angle: Edge-of-scan data can become inaccurate. The scan angle was reduced to a maximum of ±20^{o} from nadir, creating a narrow swath width and greatly reducing laser shadows from trees and buildings.

Quality GPS: Flights took place during optimal GPS conditions (e.g., 6 or more satellites and PDOP [Position Dilution of Precision] less than 3.0). Before each flight, the PDOP was determined for the survey day. During all flight times, a dual frequency DGPS base station recording at 1 second epochs was utilized and a maximum baseline length between the aircraft and the control points was less than 13 nm at all times.

Ground Survey: Ground survey point accuracy (<1.5 cm RMSE) occurs during optimal PDOP ranges and targets a minimal baseline distance of 4 miles between GPS rover and base. Robust statistics are, in part, a function of sample size (n) and distribution. Ground survey points are distributed to the extent possible throughout multiple flight lines and across the survey area.

50% Side-Lap (100% Overlap): Overlapping areas are optimized for relative accuracy testing. Laser shadowing is minimized to help increase target acquisition from multiple scan angles. Ideally, with a 50% side-lap, the nadir portion of one flight line coincides with the swath edge portion of overlapping flight lines. A minimum of 50% side-lap with terrain-followed acquisition prevents data gaps.

Opposing Flight Lines: All overlapping flight lines have opposing directions. Pitch, roll and heading errors are amplified by a factor of two relative to the adjacent flight line(s), making misalignments easier to detect and resolve.